Synthesis and structural characterization of isolable phosphine coinage metal π-complexes

Nathan D. Shapiro and F. Dean Toste†

Department of Chemistry, University of California, Berkeley, CA 94720

Edited by Jack Halpern, University of Chicago, Chicago, IL, and approved December 27, 2007 (received for review November 5, 2007)

The chemical community has recently witnessed a dramatic increase in the application of cationic gold(I)-phosphine complexes as homogeneous catalysts for organic synthesis. The majority of gold(I)-catalyzed reactions rely on nucleophilic additions to carbon–carbon multiple bonds, which have been activated by coordination to a cationic gold(I) catalyst. However, structural evidence for coordination of cationic gold(I) complexes to alkynes has been limited. Here, we report the crystal structure of a gold(I)-phosphine η^2-coordinated alkyne. Related Ag(I) and Cu(I) complexes have been synthesized for comparison. The crystallization of these complexes was enabled by tethering a labile alkyne ligand to a strongly coordinating triarylphosphine. This approach also proved applicable to crystallization of the first gold(I)-phosphine η^2-coordinated alkene.

alkyne complexes | DFT calculations | gold catalysts | homogenous catalysis | x-ray structures

The development of new synthetically useful methodology often rests on an understanding of the mechanistic underpinnings of the desired transformation. For example, the isolation and characterization of Zeise's salt, $K[PtCl_3(C_2H_4)]$, provided direct evidence for the ability of Pt(II) to remove electron density from ethylene, thereby rendering it susceptible to nucleophilic attack (1–4). This insight provided the impetus for the development of numerous platinum and palladium catalyzed reactions. In contrast, homogeneous Au(I) and Au(III) complexes have only recently emerged as highly competent and selective catalysts for the activation of π-bonds (5–8). In light of the recent synthetic advances concerning Au(I) catalysis, a thorough understanding of the mechanistic and structural basis for these reactions has lagged behind.‡

The coordination of an alkyne to a cationic Au(I)-phosphine complex represents the prototypical mechanistic starting place for Au(I)-catalyzed reactions, despite the fact that little structural evidence exists for this assertion. In fact, to date there have been no reported crystal structures of linear-phosphine-Au-(η^2-alkyne) complexes.§ Here, we report the characterization of the 14-electron Au(I)-phosphine-(η^2-alkyne) complex **1**, as well as its silver(I) and copper(I) analogues (**2** and **3**), and the cationic phosphine Au(I)-alkene complex (**4**) for comparison (Fig. 1).¶ With these structures in hand, we can begin to understand the unique ability of Au(I) complexes to serve as effective π-activation catalysts, especially in understanding why gold is often more effective than copper or silver.‖

Results and Discussion

Although Au(I)-π-complexes have traditionally been difficult to isolate and characterize, we hypothesized that these difficulties might be overcome by employing a tethered phosphine-alkyne ligand. To this end, reaction of alkynyl phosphine **5** with (dimethylsulfide)gold(I) chloride afforded the phosphinegold(I) chloride complex in 93% yield (Fig. 2). This complex was converted into cationic phosphinegold(I) complex **1** in 98% yield by abstraction of the chloride with silver hexafluoroantimonate. Crystals of complex **1** were obtained when a layered CH_2Cl_2/hexanes solution of **1** was allowed to stand at 0°C. The corresponding Ag(I) and Cu(I) complexes were obtained in quantitative yields by the reaction of ligand **5** directly with cationic metal precursors. The structures of the complexes **1**–**3** were firmly established by x-ray crystallographic analysis (Figs. 3 and 4). In all cases, solvent molecules and counterions are completely separated from the cationic metal centers. The Au(I) and Ag(I) complexes **1** and **2** are structurally analogous dimers, both displaying pseudo-linear geometry about the metal.†† Although, the dimeric structure of **1** and **2** was unexpected, it is not surprising considering the structure of the ligand and the preferred linear Au(I)-coordination geometry. In contrast, the Cu(I) complex **3** is monomeric, with pseudo-trigonal planar geometry about copper.

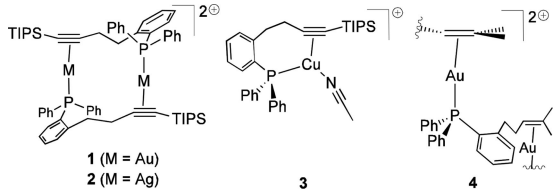

Fig. 1. Schematic representations of the coinage metal alkyne complexes **1** (M = Au), **2** (M = Ag), and **3**, together with a portion of Au-alkene coordination polymer **4**.

Finally, a crystal structure of the first (η^2-alkene)-Au(I)-phosphine complex **4** was obtained using an analogous alkene-tethered phosphine ligand (15–19) (Fig. 5). In agreement with previous calculations, the Au(I)-alkene bond is longer than the

Author contributions: N.D.S. and F.D.T. designed research; N.D.S. performed research; N.D.S. and F.D.T. analyzed data; and N.D.S. and F.D.T. wrote the paper.

The authors declare no conflict of interest.

This article is a PNAS Direct Submission.

Data deposition: The crystallographic data have been deposited in the Cambridge Structural Database, Cambridge Crystallographic Data Centre, Cambridge CB2 1EZ, United Kingdom [CSD references nos. CCDC-676997 (**1**), CCDC-676998 (**2**), CCDC-676999 (**3**), and CCDC-677000 (**4**)]. These data can be obtained free of charge from the Cambridge Crystallographic Data Centre via www.ccdc.cam.ac.uk/data_request/cif.

†To whom correspondence should be addressed. E-mail: fdtoste@berkeley.edu.

‡Most previous mechanistic investigations of Au(I)-catalyzed reactions have not involved the isolation of Au-containing intermediates; for an exception, see ref. 9.

§Previous examples of Au-(η^2-alkyne)-containing compounds that have been characterized by x-ray crystallography include a gold(I)-[2]catenane containing a linear (η^1-alkyne)-Au-(η^2-alkyne) moiety (10), several trigonal planar Au(I) complexes coordinated to organometallic 1,4-diynes (11, 12), two trigonal planar strained cycloheptyne-Au(I) complexes (13), and a supramolecular complex containing a linear (η^2-alkyne)-Au-(η^2-alkyne) moiety (14). For a linear N-heterocyclic carbene-Au-(η^2-alkyne) that has been characterized by NMR and IR spectroscopy, see ref. 9.

¶For a review of η^2-alkyne Cu(I) and Ag(I) compounds, see ref. 15. For linear phosphine-Au(I)-(η^2-arene) complexes, see ref. 16. For recent 16-electron trigonal planar Au(I)-(η^2-alkene) complexes, see refs. 19–21.

‖Reactions involving Cu-catalyzed electrophilic π-bond activation are rare; for examples, see refs. 20–24.

††In the case of the Ag(I) dimer there is a center of inversion, whereas the two halves of the Au(I) complex are pseudo-symmetric.

This article contains supporting information online at www.pnas.org/cgi/content/full/0710500105/DC1.

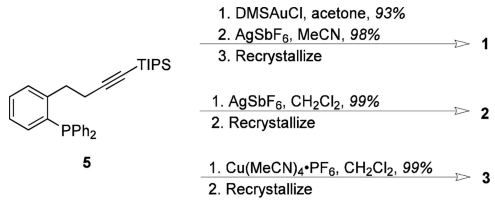

Fig. 2. Synthesis of coinage metal alkyne complexes **1–3**, from alkynyl phosphine **5**.

Au(I)-alkyne bond, despite the fact that the former is calculated to be stronger (25, 26).

A comparison of the some relevant structural features of **1–3** is given in Table 1. The Cu(I)-bound alkyne has the smallest C(1)-C(2)-C(3) and C(2)-C(1)-Si(1) angles [159.8(3)° and 159.5(2)°] and the lowest stretching frequency (2,020 cm^{-1}). In contrast, the Au(I)- and Ag(I)-bound alkynes exhibit significantly less distortion from linearity [C(1)-C(2)-C(3) angles of 167.2(6)° and 172.9(3)°, respectively]. The observed deviations of the alkyne from linearity correspond well to a decrease in the bond's stretching frequency. It is also important to note that in both the Au(I) and Ag(I) complexes (**1** and **2**), the metal center is significantly "slipped" to one side of the π-bond. Previous research suggests that such $\eta^2 \rightarrow \eta^1$ migration should accompany an increase in ligand electrophilicity (27, 28). In contrast, the Cu-alkyne complex is highly symmetrical [2.029(2) vs. 2.024(2) Å],

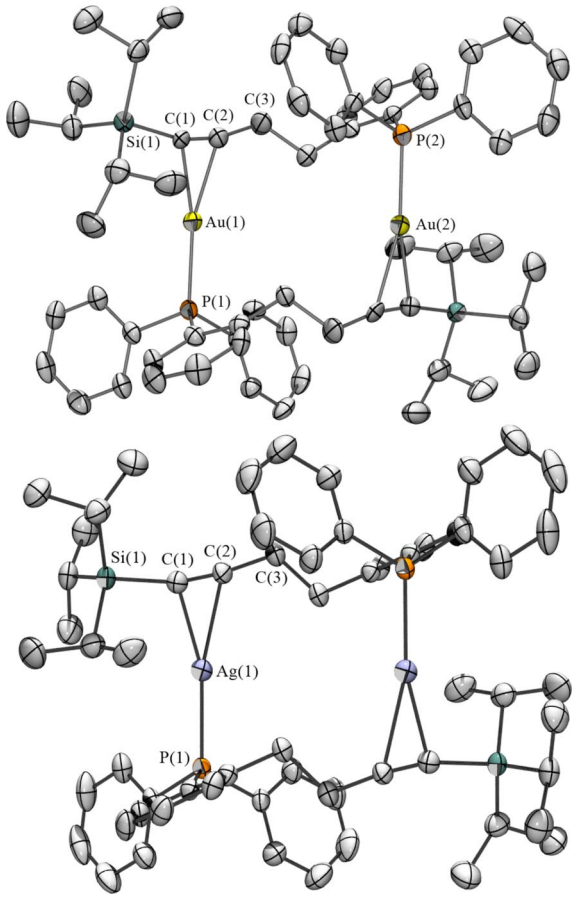

Fig. 3. ORTEP drawings of the Au- and Ag-alkyne complexes **1** and **2**, respectively, shown as 50% ellipsoids. Hydrogens, solvent, and counterions (SbF_6) omitted for clarity. For selected bond lengths and angles see Table 1.

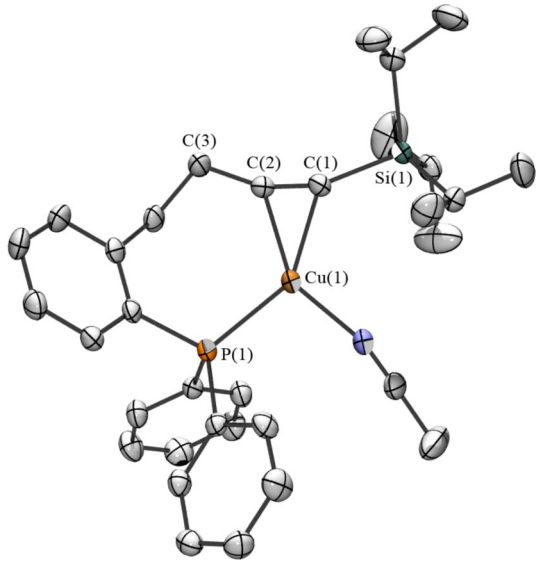

Fig. 4. ORTEP-drawing of the Cu-alkyne complex **3**, shown as 50% ellipsoids. Hydrogens, solvent, and counterion (PF_6) are omitted for clarity. For selected bond lengths and angles, see Table 1.

although this may be a result of the altered geometry and electron count of this complex.

Experimentally, we have observed that Au(I) complexes are generally superior π-activation catalysts, especially when compared with analogous Cu(I) and Ag(I) complexes. Intuitively, the superior catalytic activity of Au(I) in these reactions suggests that Au(I)-coordinated π-bonds are more activated toward nucleophilic attack than π-bonds that are coordinated to Ag(I) or Cu(I). Under the Dewar–Chatt–Duncanson bonding model, this further suggests increased π-to-metal σ-donation to gold and/or decreased metal-to-π^* back-donation from gold (29, 30). Therefore, we sought to compare the relative importance of these two types of bonding for complexes **1–3**. The situation is complicated by the fact that both π-to-metal σ-donation and metal-to-π^* back-bonding elongate and distort a coordinated π-bond. As a result, one cannot directly correlate the degree of alkyne distortion with the degree of metal-to-π^* back-donation. To circumvent these problems, we turned to DFT calculations (17, 31–35).

Beginning with the crystal structure of Au(I) complex **1**, we initially simplified the structure to monomeric triphenylphosphine-metal-alkyne complex **1b** (Fig. 6). The experimental geometric features were well produced with the B3PW91/LANL2DZ(Au), LANL2DZdp(Si,P), ccpVDZ(C,H) level of theory (Table 1) [for further details on the synthesis and characterization of complexes **1–4**, see supporting information (SI) *Appendix*]. Importantly, this indicates that the geometry of

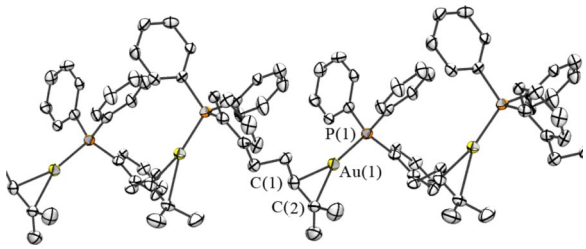

Fig. 5. ORTEP drawing of the Au-alkene complex **4**, shown as 50% ellipsoids. Hydrogens, solvent, and counterions (SbF_6) are omitted for clarity. Selected bond lengths (Å): P(1)-Au(1), 2.272(3); Au(1)-C(1), 2.250(10); and Au(1)-C(2), 2.34(1).

Table 1. Selected bond lengths (Å), bond angles (°), and IR stretching frequencies (cm^{-1})—experimental and calculated

Entry†	Parameter	**1** (M = Au)‡	**2** (M = Ag)	**3** (M = Cu)
1a	d C(1)-C(2)	1.221(8)	1.211(4)	1.229(4)
1b		1.258	1.252	1.265
2a	∠C(1)-C(2)-C(3)	167.2(6)	172.9(3)	159.8(3)
2b		171.0	173.6	158.9
3a	∠Si(1)-C(1)-C(2)	164.4(5)	165.3(3)	159.5(2)
3b		160.0	160.8	161.3
4a	νC(1)≡C(2)§	2053	2095	2020
4b		2068	2100	2014
5a	d M(1)-C(1)	2.197(5)	2.294(3)	2.029(2)
5b		2.249	2.292	2.077
6a	d M(1)-C(2)	2.270(5)	2.445(3)	2.024(2)
6b		2.386	2.493	2.070
7a	d P(1)-M(1)	2.271(1)	2.3934(8)	2.2571(7)
7b		2.337	2.431	2.338

†*n*a, experimental value; *n*b, calculated value.
‡Data from one half of the unsymmetrical Au-dimer is shown. For the other half, see *SI Appendix*.
§The $\nu_{C(1)\equiv C(2)}$ of the free ligand is 2,171 cm^{-1}.

the metal center in **1** is not significantly influenced by the constraints of crystallization. The structures of **2** and **3** were trimmed and optimized similarly; the experimental and calculated values are compared in Table 1. The same structural trends were observed in both the calculated and experimental geometries. With these optimized geometries in hand, we turned to natural bond order calculations to investigate the nature of the metal-alkyne bond (Table 2) (for similar studies, see refs. 25 and 31–34). Second-order perturbative analysis revealed that π-to-metal σ-donation is of the largest magnitude for Au (56.6 kcal/mol), as is metal-to-π^* back-donation (13.3 kcal/mol). For all three metals, σ-donation to the metal dominates, augmenting the electrophilicity of the alkyne, although the difference of the two bonding interactions is the largest for Au. These calculations also provide further insight into the observed distortion of the Cu(I)-bound alkyne. Noting that the calculated Cu-alkyne orbital interaction energies underestimate the degree of distortion suggests that some of the distortion of the Cu-bound alkyne may be due to geometrical constraints of that system.

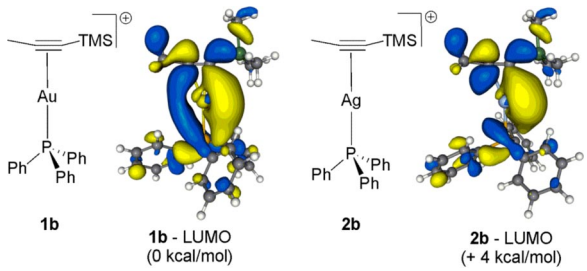

Fig. 6. Structures of **1b** and **2b** along with the calculated lowest unoccupied molecular orbitals (LUMOs) and corresponding energies.

Table 2. Natural bond order orbital interaction energies

Parameter	**1b** (M = Au)	**2b** (M = Ag)	**3b** (M = Cu)
$\pi \rightarrow$ M	56.6	38.5	46.9
M $\rightarrow \pi^*$	13.3	6.4	12.0
Difference	43.3	32.1	34.9

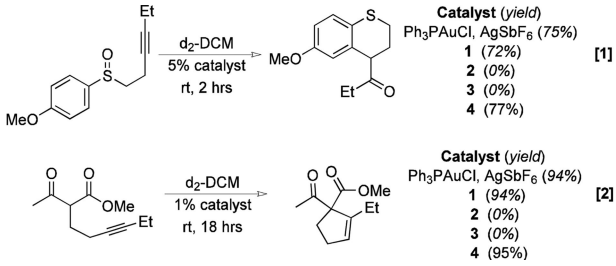

Fig. 7. Reactivity of coinage metal complexes **1**–**4** in typical gold(I)-catalyzed reactions.

In addition to NBO analysis, we also examined the frontier molecular orbitals of **1b** and **2b** (Fig. 6).‡‡ As expected, the lowest unoccupied molecular orbitals (LUMOs) contain the π^*-metal interaction. Furthermore, the LUMO of **1b** was calculated to be 4 kcal/mol lower in energy than the LUMO of **2b**. Although the energies of unoccupied orbitals must be considered with caution, this result is again qualitatively in agreement with Au(I) being a superior π-activation catalyst.

In agreement with the above claims, we have also found that complexes **1** and **4** are active in typical gold(I)-catalyzed reactions, whereas **2** and **3** are not (Fig. 7) (36–38). It is worth mentioning that phosphine-Au(I)-chloride complexes (16-electron complexes upon alkyne coordination) are typically much less catalytically active than their cationic congeners. Thus, Ph_3PAuCl is typically activated by addition of a silver salt (such as $AgSbF_6$), which serves to remove the chloride ligand and replace it with a less coordinating counteranion. Complexes **1** and **2** represent 14-electron Au(I) and Ag(I) complexes, whereas similar crystallization conditions result in 16-electron Cu(I) complex **3**. Furthermore, the observation that the alkene complex **4** is also catalytically active supports the assumption that coordination of cationic gold(I) complexes to π-bonds is reversible and that the observed selectivity for alkynes in many gold-catalyzed reactions does not arise as a result of preferred bonding to the alkyne.

In summary, we have isolated and characterized, by x-ray crystallography, linear (η^2-alkyne)- and (η^2-alkene)-Au(I)-phosphine complexes. The isolation of these complexes was enabled by covalently linking kinetically labile alkenes and alkynes to triphenylphosphine.

Experimental Procedures

1. To a solution of the corresponding phosphine-AuCl complex. (37 mg, 0.053 mmol) in d_3-acetonitrile (0.4 ml) was added $AgSbF_6$ (18 mg, 0.053 mmol). Silver chloride precipitated immediately, providing a solution of the corresponding cationic phosphine-Au-acetonitrile complex. ^{1}H NMR (400 MHz, d_3-MeCN) δ 7.64–7.51 (m, 12H), 7.27–7.22 (m, 1H), 6.80 (dd, 1H, J = 13.4, 7.8 Hz), 3.12 (t, 2H, J = 7.3 Hz), 2.51 (t, 2H, J = 7.3 Hz), 1.08–0.92 (m, 21H). ^{13}C NMR (100 MHz, d_3-MeCN) δ 144.5 (d, J = 12 Hz), 135.3 (d, J = 14 Hz), 134.2 (d, J = 9 Hz), 133.5 (d, J = 2 Hz), 133.2, 131.8 (d, J = 9 Hz), 130.6 (d, J = 12 Hz), 128.4 (d, J = 67 Hz), 128.1 (d, J = 10 Hz), 126.8 (d, J = 62 Hz), 108.9, 82.5, 34.3 (d, J = 12 Hz), 21.1, 19.0, 11.9. ^{31}P NMR (162 MHz, d_3-MeCN) δ 24.44.

This solution was then filtered through celite and concentrated *in vacuo*. The resulting solid (49 mg, 98% yield) was dissolved in dichloromethane and again filtered through celite. X-ray quality crystals were grown by layering the resulting solution with hexanes. IR: 2,053, 1,472, 1,439, 1,102, 883 cm^{-1}. Attempted NMR analysis of the crystals was hampered by broad signals and instability of the sample to disproportionation. ^{1}H NMR (400 MHz, $CDCl_3$) δ 7.64–7.50 (m, 12H), 7.32 (m, 1H), 6.89 (m, 1H), 3.4–3.1 (m, 4H), 1.20–0.90 (m, 21H). ^{31}P NMR (162 MHz, $CDCl_3$) δ 29.3. HRMS (FAB) calculated for $[C_{31}H_{39}PSiAu]^+$ 667.2224, found 667.2218.

‡‡The frontier molecular orbitals of **3b** are similar. However, a comparison of **3b** with **1b** and **2b** is less informative because of the altered electron count and geometry about the Cu(I) center.

CHEMISTRY

X-Ray Data. $C_{31.5}H_{40}F_6SiPClSbAu$, $M_r = 945.88$, triclinic, space group $P\bar{1}$ (#2); $a = 13.963(2)$, $b = 14.920(2)$, $c = 18.703(2)$ Å, $\alpha = 69.422(1)$, $\beta = 77.264(2)$, $\gamma = 75.161(2)°$, $V = 3489.2(7)$ Å^3, $Z = 4$; $\rho_{calcd} = 1.80$ g/cm^3, μ (Mo-Kα) = 51.97 cm^{-1}, Mo-Kα radiation ($\lambda = 0.71069$ Å), 153 K, $2\theta_{max} = 52.0°$, 9,559 unique reflections of 31,450 measured, $R_{int} = 0.028$, $R = 0.032$, $Rw = 0.035$. Crystal dimensions: $0.08 \times 0.08 \times 0.17$ mm.

ACKNOWLEDGMENTS. We thank Dr. Frederick J. Hollander of the Berkeley CHEXray facility for solving the x-ray crystal structures of compounds **1–4**, and Prof. O. Eisenstein (Université Montpellier II) for helpful discussions. This work was supported by National Institute of General Medical Sciences Grant RO1 GM073932, Merck Research Laboratories, Bristol-Myers Squibb, Amgen, Boehringer Ingelheim, and Novartis for funding. N.D.S. gratefully acknowledges a graduate fellowship from Eli Lilly.

1. Zeise WC (1827) *Poggendorff's Ann Phys* 9:632.
2. Wunderlich JA, Mellor DP (1954) *Acta Crystallogr* 7:130.
3. Jarvis JAJ, Kilbourn BT, Owsten PG (1971) *Acta Crystallogr B* 27:366–372.
4. Love RA, Koetzle TF, Williams GJB, Andrews LC, Bau R (1975) *Inorg Chem* 14:2653–2657.
5. Gorin DJ, Toste FD (2007) *Nature* 446:395–403.
6. Jiménez-Núñez E, Echavarren AM (2007) *Chem Commun*, 333–346.
7. Fürstner A, Davies PW (2007) *Angew Chem Int Ed* 46:3410–3449.
8. Hashmi ASK (2007) *Chem Rev* 107:3180–3211.
9. Akana JA, Bhattacharyya KX, Müller P, Sadighi JP (2007) *J Am Chem Soc* 129:7736–7737.
10. Mingos DMP, Yau J, Menzer S, Williams DJ (1995) *Angew Chem Int Ed* 34:1894–1895.
11. Lang H, Köhler K, Zsolnai L (1996) *Chem Commun*, 2043–2044.
12. Köhler K, Silverio SJ, Hyla-Krypsin I, Gleiter R, Zsolnai L, Driess A, Huttner G, Lang H (1997) *Organometallics* 16:4970–4979.
13. Schulte P, Behrens U (1998) *Chem Commun*, 1633–1634.
14. Yip S, Cheng EC, Yuan L, Zhu N, Yam VW (2004) *Angew Chem Int Ed* 43:4954–4957.
15. Lang H, Köhler K, Blau S (1995) *Coord Chem Rev* 143:113–168.
16. Herrero-Gómez E, Nieto-Oberhuber C, López S, Benet-Buchholz J, Echavarren AM (2006) *Angew Chem Int Ed* 45:5455–5459.
17. Cinellu MA, Minghetti G, Cocco F, Stoccoro S, Zucca A, Manassero M, Arca M (2006) *J Chem Soc Dalton Trans*, 5703–5716.
18. Dias HVR, Wu J (2007) *Angew Chem Int Ed* 46:7814–7816.
19. Dias HVR, Fianchini M, Cundari TR, Campana CF (2007) *Angew Chem Int Ed* 46:556–559.
20. Bouyssi D, Monteiro N, Balme G (1999) *Tetrahedron Lett* 40:1297–1300.
21. Asao N, Nogami T, Lee S, Yamamoto Y (2003) *J Am Chem Soc* 125:10921–10925.
22. Asao N, Kasahara T, Yamamoto Y (2003) *Angew Chem Int Ed* 42:3504–3506.
23. Patil NT, Wu H, Yamamoto Y (2005) *J Org Chem* 70:4531–4534.
24. Fehr C, Farris I, Sommer H (2006) *Org Lett* 8:1839–1841.
25. Nechaev MS, Rayón VM, Frenking G (2004) *J Phys Chem A* 108:3134–3142.
26. Yamamoto Y (2007) *J Org Chem* 72:7817–7831.
27. Eisenstein O, Hoffmann R (1981) *J Am Chem Soc* 103:4308–4320.
28. Wright LL, Wing RM, Rettig MF (1982) *J Am Chem Soc* 104:610–612.
29. Dewar M (1951) *Bull Soc Chim Fr* 18:C71–C79.
30. Chatt J, Duncanson LA (1953) *J Chem Soc*, 2939–2947.
31. Ziegler T, Rauk A (1979) *Inorg Chem* 18:1558–1565.
32. Hertwig RH, Koch W, Schröder D, Schwarz H, Hrušák J, Schwerdtfeger PJ (1996) *Phys Chem* 100:12253–12260.
33. Kim CK, Lee KA, Kim CK, Lee B, Lee HW (2004) *Chem Phys Lett* 391:321–324.
34. Tai H-C, Krossing I, Seth M, Deubel DV (2004) *Organometallics* 23:2343–2349.
35. Nakanishi W, Yamanaka M, Nakamura E (2005) *J Am Chem Soc* 127:1446–1453.
36. Shapiro ND, Toste FD (2007) *J Am Chem Soc* 129:4160–4161.
37. Kennedy-Smith JJ, Staben ST, Toste FD (2004) *J Am Chem Soc* 126:4526–4527.
38. Staben ST, Kennedy-Smith JJ, Toste FD (2004) *Angew Chem Int Ed* 43:5350–5352.